IEEE Access
Multidisciplinary | Rapid Review | Open Access Journal

Received November 24, 2020, accepted November 30, 2020, date of publication December 7, 2020,
date of current version December 28, 2020.

Digital Object Identifier 10.1109/ACCESS.2020.3042756

Usability of a 5G Fronthaul Based on a DML and External Modulation for M-QAM Transmission Over Photonically Generated 40 GHz

LUIS VALLEJO[1], (Member, IEEE), BEATRIZ ORTEGA[1], (Member, IEEE), DONG-NHAT NGUYEN[2], (Member, IEEE), JAN BOHATA[2], VICENÇ ALMENAR[1], AND STANISLAV ZVANOVEC[2], (Senior Member, IEEE)

[1]Instituto de Telecomunicaciones y Aplicaciones Multimedia, Universitat Politecnica de Valencia, 46022 Valencia, Spain
[2]Department of Electromagnetic Field, Faculty of Electrical Engineering, Czech Technical University in Prague, 166 27 Prague, Czech Republic

Corresponding author: Luis Vallejo (luivalc2@iteam.upv.es)

This work was supported in part by the Generalitat Valenciana under Grant PROMETEO 2017/103, in part by the Ministerio de Ciencia, Innovación y Universidades under Grant FOCAL RTI2018-101658-B-I00, in part by the Ministerstvo Prumyslu a Obchodu under Grant FV40089, and in part by the European Cooperation in Science and Technology under Grant CA16220.

ABSTRACT In this paper, we numerically and experimentally present the bandwidth constraints of a cost-effective 5G mobile fronthaul based on a directly-modulated laser for data modulation and a Mach-Zehnder modulator-based optical double sideband with carrier suppression scheme for optical millimeter wave (mmW) signal generation. The effect of chirp, fiber dispersion and a combination of both on different bandwidth M-Quadrature Amplitude Modulation (M-QAM) signals, i.e. M = 4, 16 and 64, at 40 GHz has also been investigated. Simulation results are first carried out to evaluate the impact of higher chirp of the directly-modulated laser on the link performance as a function of modulation format and signal bandwidth. We then experimentally demonstrate the same scheme transmitting M-QAM signals with bandwidths ranging from 50 to 1000 MHz over a 10 km long single mode fiber. Both experimental and simulation results show that larger signal bandwidths lead to higher optical power penalties due to the combined effect with the error vector magnitudes (EVMs), however still satisfying the required limits of 3GPP standard for all QAM signals. Experimental measurements also show the feasibility of including free space optics links in the optical distribution network with no further significant penalties. Finally, a multiband signal (three-band) transmission is demonstrated leading to an increase of the total bitrate with the measured EVMs are well below the EVM requirement.

INDEX TERMS Directly-modulated laser (DML), mobile fronthaul network, radio-over-fiber (RoF), photonic millimeter wave generation, fiber-wireless, 5G networks.

I. INTRODUCTION

Nowadays, broadband mobile services, such as cloud access, 4K/8K high definition video, augmented virtual reality, online gaming or social networking require the deployment of the 5th generation (5G) mobile communications providing high bandwidth and low latency connectivity [1].

Centralized cloud-radio access network (C-RAN) [2] is the preferred architecture for 5G networks due to the centralization of the baseband units (BBU) in a central pool which is connected to the remote radio heads (RRH) by the mobile fronthaul network (MFH). Since the BBU pool includes most of the signal processing and the RRH mainly performs RF/baseband conversion, such architecture offers reduced operational and capital expenditure. Conventional MFHs have employed the digital fiber-optic interfaces such as common public radio interface (CPRI), but 5G networks traffic would exceed hundreds of Gb/s [3] and further functions splitting is required in the enhanced CPRI (eCPRI) interface [4]. However, analog radio-over-fiber (RoF) approach combined with optical distribution network (ODN) technology offers a scalable and flexible solution with increased spectral efficiency and transmission capacity by using transceivers with a bandwidth of a few Gb/s [5], [6].

The associate editor coordinating the review of this manuscript and approving it for publication was Sukhdev Roy.

Moreover, the spectral congestion of lower microwave spectral region is the motivation for exploiting higher frequency bands (25-170 GHz) [7]–[10], i.e. millimeter wave (mmW) frequencies, which however suffer from the high propagation loss and thus cannot be used for long range communication.

Moreover, multiband mmW over RoF is a promising approach to provide multiple services simultaneously [11]. Several schemes of multiband signals have been demonstrated [12] by considering base, microwave and mmW bands to carry one service. However, other examples in the literature show an optical multiband transmission with each band carrying an individual service, such as three bands of Quadrature Phase-Shift Keying (QPSK) Orthogonal Frequency Division Multiplexing (OFDM) over 30 GHz [13], a 720P HD video combined with 16-QAM data signal over 60 GHz [14] or OFDM, IEEE 802.11ah and LTE-A services over 92 GHz [15].

Considering the reduced size of 5G network cells down to femto-cells, operating in the mmW frequency band, the large number of cell sites need to be therefore connected to the MFH, while cost-effective optical transmitters are critical for massive deployment. Previous works have demonstrated the feasibility of directly-modulated lasers (DML) for transmitting 1 Gb/s at 24 GHz using QPSK modulation [16], data transmission of 24 carriers with 100 MHz bandwidth filtered-OFDM (f-OFDM) [17], a 100 MHz bandwidth signal transmitted at 24 GHz [18] or a 10 Gb/s 16-Quadrature Amplitude Modulation (QAM) OFDM at 60 GHz [19]. Moreover, the use of linear externally modulated lasers at the BBU allowed a multiband operation up to 12 Gb/s over the MFH link in [20] and an electro-absorption modulated (EAM) laser, in spite of its inherent nonlinearities, was employed to transmit of 24 OFDM bands of 100-MHz-bandwidth as shown in [17]. The comparison between different transmitters at 25 GHz for RoF systems including DML, EAML and MZM has been recently published in [21]. Noteworthy, very recent work demonstrates the monolithic integration of multiple DMLs for 5G RoF systems [22], opening new opportunities for infrastructure sharing in 5G networks.

However, both the generation and transport of mmW signals have become a challenge for the new generation of wireless communication networks. Many different approaches have been previously demonstrated for optical mmW signal generation, such as those employing dual-mode lasers [23], mode-locked lasers [24], [25], nonlinear effects [26]–[28] or external modulation [29]. The use of different bias operation point in the external modulators leads to optical double sideband (ODSB), optical single sideband (OSSB), or alternatively optical carrier suppression (OCS) modulation schemes [2]. In particular, the OCS approach based on optical frequency multiplication between the externally modulated sidebands is very convenient in terms of flexibility and simplicity, and it allows achieving frequency doubling, quadrupling and up to 8-tupling [29] with a significant reduction of the electric bandwidth requirements. Moreover, the external modulator in the BBU pool is part of the optical infrastructure shared among multiple RRHs, which significantly contributes to reduce the overall cost [30].

Nevertheless, besides the inherent impairments of an analog optical link, including the impact of chromatic dispersion and noise, the OCS scheme leads to high frontend nonlinearity due to the MZM operation point at the minimum transmission. Moreover, another MZM is also typically used to modulate the optical carrier with the data signal in RoF schemes. Different configurations of MZM have been demonstrated, such as two cascade MZMs [29], [31], dual parallel MZM [32] or a single MZM [24], [23]. In this context, the DML is an attractive approach which saves insertion losses and costs due to the second external modulator, although the impact of chromatic dispersion of chirped signals needs to be addressed.

In the literature, different optical frontends have been proposed for RoF networks using DML for baseband data transmission over photonically mmW generated signals, either using a broadband external modulator to up-convert the signals or using an electrical mixer to up-convert the baseband signal before direct modulation of a broadband laser and then, suppressing the optical carrier by filtering [33]. Recent papers report on direct modulation of the up-converted QPSK electrical signal in combination with wavelength selective filtering [34] or the use of several injection locking systems to transmit several Gb/s OFDM data over 60 GHz [19], [35].

In this paper, we employ a cost-effective MFH with a hybrid link including a standard single-mode fiber (SSMF) and free space optics (FSO) channel based on DML for data modulation and CS-MZM for optical mmW generation. For the sake of obtaining the usability in terms of bandwidth, theoretical and experimental evaluation of the effect of fiber dispersion and chirp over different M-QAM signals bandwidth is presented for the first time to the authors' knowledge. Finally, the transmission performance of the single and multiband QAM signals is also provided over the proposed system.

The rest of the paper is structured as follows: Section II includes the theoretical and simulation results and Section III shows the experimental setup and system characterization measurements. Section IV and Section V present the experimental results of single and multiband transmission performance, respectively. Finally, Section VI summarizes the main conclusions of the paper.

II. THEORETICAL SIMULATIONS

In this section, simulations have been carried out to characterize the system performance of the M-QAM signal transmission based on DML and external modulation for mmW up-conversion using an optical frequency multiplication (OFM) technique. OptiSystem and MATLAB software tools have been employed to evaluate the effect of laser chirp and fiber dispersion on the transmitted signals in order to assess the bandwidth limitations of such system and,

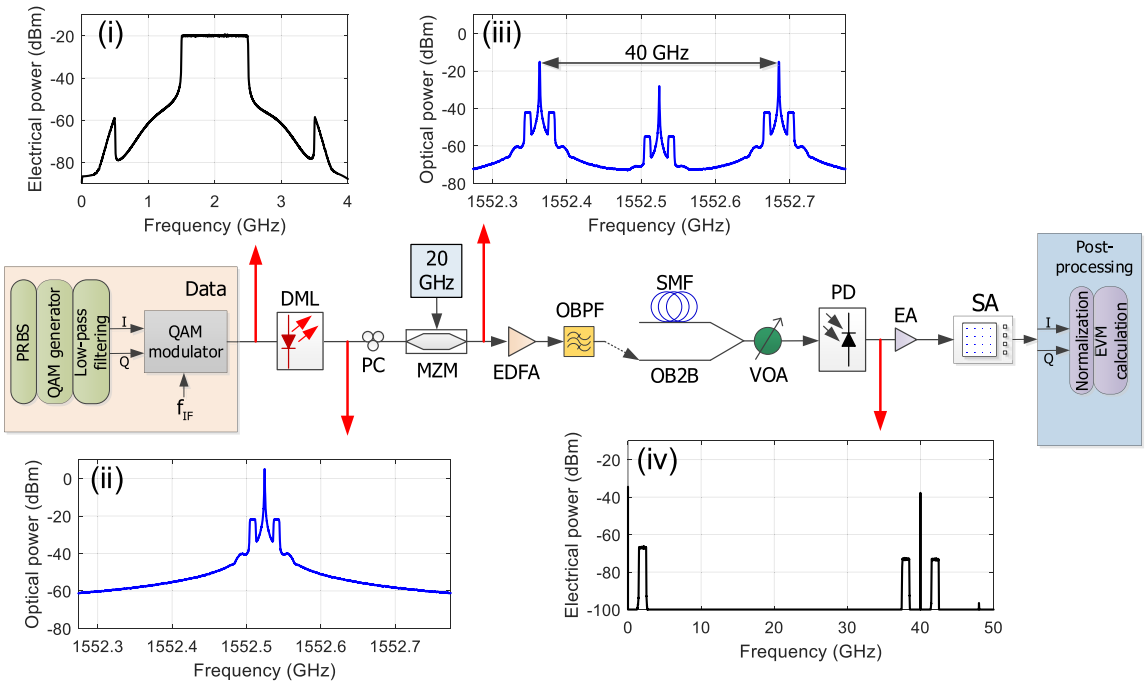

FIGURE 1. Simulated schematic of the M-QAM DML and external modulation for mmW up-conversion based on OFM. Insets: (i) and (iv) Electrical spectra of the modulation data and after opto-electronic conversion (RBW = 10 MHz) and, (ii) and (iii) Optical spectra at the DML and MZM output (RBW = 0.001 nm). PRBS: pseudorandom binary sequence, QAM: quadrature amplitude modulation, DML: directly-modulated laser, PC: polarization controller, MZM: Mach-Zehnder modulator, EDFA: erbium doped fiber amplifier, OBPF: optical band pass filter, OB2B: optical back-to-back, SSMF: standard single-mode fiber, VOA: variable optical attenuator, PD: photodetector, EA: electrical amplifier, SA: signal analyzer, EVM: error vector magnitude.

therefore, about its future deployment in the fronthaul of 5G networks.

The schematic of the optical MFH employed along the paper is depicted in Fig. 1. A distributed feedback (DFB) laser emits an optical carrier which is directly modulated by an electrical M-QAM data signal of Δf bandwidth combined with an intermediate frequency (IF) signal at 2 GHz. The inset (i) of Fig. 1 shows the electrical spectra of 2 GHz bandwidth modulating signal. The direct modulation causes signal chirp, which interplays with chromatic dispersion of the optical fiber and would contribute to the composite second order (CSO) distortions in large bandwidth systems [17]. Furthermore, relative intensity noise (RIN) in the laser diode also causes signal degradation, which is added to the thermal and shot noise at the photodetector (PD) side. The signal is then launched into an MZM, which is biased at the null transmission point and driven by a single-tone RF signal at 20 GHz, which is the half value of the desired mmW frequency at the RRH. Inset (ii) of Fig. 1 depicts the optical spectra of the directly modulated signal and inset (iii) shows the modulated signal at the output of the external modulator exhibiting 13.1 dB of carrier suppression ratio. Therefore, CS modulation is obtained and the effect of chromatic dispersion is reduced. However, such modulation scheme is strongly nonlinear, and additional distortion terms contribute to signal degradation unless moderate bandwidth and low-level amplitude are employed to guarantee the system feasibility. Further optical amplification to compensate losses and filtering to reduce the amplified spontaneous emission noise are held before detection. The optical back-to-back (OB2B) characterization as a benchmark is obtained by a direct connection to the PD through a variable optical attenuator (VOA). Inset (iv) of Fig. 1 shows the spectrum of the recovered signal after photodetection, where mmW signal with central frequency at 40 GHz is generated by beating both sidebands at 20 GHz, so the data bands appear at 38 and 42 GHz. In the following, an optical fiber link is included before the VOA to implement the penalty induced by 10 km long fiber propagation, which is typical MFH distance. The system parameters employed in the simulations are detailed in Table 1.

The performance of the RoF-based MFN employing a DML is mainly limited by the interplay between DML adiabatic chirp and fiber chromatic dispersion [17]. The instantaneous frequency shift of DML emitting at frequency ν can be expressed in terms of the transient and adiabatic components of chirp:

$$\Delta\nu = -\frac{\alpha}{4\pi}\left(\frac{d}{dt}ln\left[P\left(t\right)\right] + kP\left(t\right)\right) \tag{1}$$

where $P\left(t\right)$ is the instantaneous optical power of the DML, α is the linewidth enhancement factor, which is responsible for the transient chirp, and k is the adiabatic chirp coefficient.

Provided first-order dispersion is only considered, the general transfer function of a small signal intensity modulated

and directly detected (IM/DD) dispersive channel is given by [36]:

$$H_{DML}(w) = \sqrt{\alpha^2 + 1}\, cos\left(\theta + tan^{-1}\alpha\right) + j\frac{\alpha k P_0}{w}\, sin\theta \quad (2)$$

where the angular frequency is $w = 2\pi f$, P_0 is the output power of the laser and θ is related to the phase variation induced by the chromatic dispersion.

Since the directly modulated signal in Fig. 1 is up-converted to an RF signal, $f_{RF} = 20GHz$ ($w_{RF} = 2\pi f_{RF}$), using OCS modulation, the dispersion term in this case will be given by [36]:

$$\theta = \frac{LD\lambda_0^2 w(2w_{RF} + w)}{4\pi c} \quad (3)$$

where D is the chromatic dispersion coefficient, λ_0 is the wavelength of the optical source, L is the transmission distance and c is the speed of light in vacuum.

Fig. 2(a) and (b) show the frequency response due to laser chirp and fiber dispersion obtained from (2) and simulation of the system depicted in Fig. 1 using 10 and 20 km fiber link, respectively.

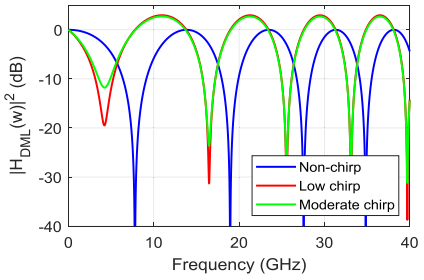

(a)

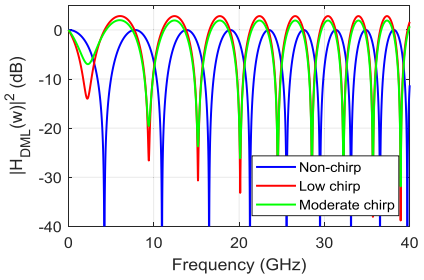

(b)

FIGURE 2. Theoretical and simulated channel transfer function (scattering parameter S_{21}) for different chirp parameters: (a) 10 km fiber link and (b) 20 km fiber link.

As depicted in Fig. 2(a) in the simulated system, the −3 dB bandwidth is 4.2 GHz when non-chirped signal is transmitted over 10 km fiber link whereas bandwidth is reduced down to 1.5 and 1.4 GHz with $\alpha = 1$ and low (k= 4 GHz/mW) and moderate (k= 10 GHz/mW) adiabatic chirp, respectively, according to Table 1. These values have been considered as typical in real devices [17]. The system response shows notches at 4.1 GHz due to the transient chirp. The adiabatic chirp has an impact on the channel response since the frequency notches caused by the adiabatic chirp are compensated by the transient chirp [5]. Fig. 2(b) shows a similar impact on the transfer function when the chirped signal is transmitted over 20 km fiber link where −3 dB bandwidth decreases down to 0.8 GHz. Since the laser chirp is related to the bias current and modulation amplitude, further optimization can be done to obtain higher performance links [37].

TABLE 1. Simulations parameters.

Parameter	Value
Laser	
• Wavelength	1552.52 nm
• Output power	5.45 dBm
• RIN	-155 dB/Hz
• Bandwidth	$5\log_2(M)\sqrt{3}\,\Delta f$
• Linewidth	10 MHz
• Linewidth enhancement factor	1
• Chirp	Null: 0 GHz/mW Low: 4 GHz/mW Moderate: 10 GHz/mW High: 15 GHz/mW
Modulation data	
• Modulation format	4-, 16-, 64-QAM
• Electrical power	0 dBm
RF signal	
• Frequency	20 GHz
• Electrical power	18 dBm
MZM	
• Switching bias voltage	4 V
• Switch RF voltage	4 V
• Insertion loss	3 dB
• Bias voltage	4 V
EDFA	
• Gain	14 dB
• Noise figure	2 dB
OBPF	
• Wavelength	1552.52 nm
• Bandwidth	0.64 nm
• Band rejection	60 dB
• Insertion loss	1.3 dB
Fiber	
• Length	10 or 20 km
• Attenuation	0.2 dB/km
• Chromatic dispersion	16.75 ps/(nm.km)
PD	
• Responsivity	0.6 A/W
• Dark current	5 nA
• Thermal noise	50e-12 pA/Hz$^{-1/2}$
EA	
• Gain	35 dB

A. IMPACT OF DIFFERENT 4/16/64-QAM SIGNAL BANDWIDTHS

In the following, the error vector magnitude (EVM) of the transmission system was evaluated as the performance and EVM threshold levels were set as those corresponding to an OFDM signal [38], as a worst case reference. Fig. 3 shows the obtained EVM when OB2B is simulated for 4-, 16- and 64-QAM signals with 1, 1.5 and 3 GHz bandwidths. Fig. 3(a) further depicts the obtained EVM for a 4-QAM signal. At 17.5% EVM threshold level [38], a 0.7 dB increase

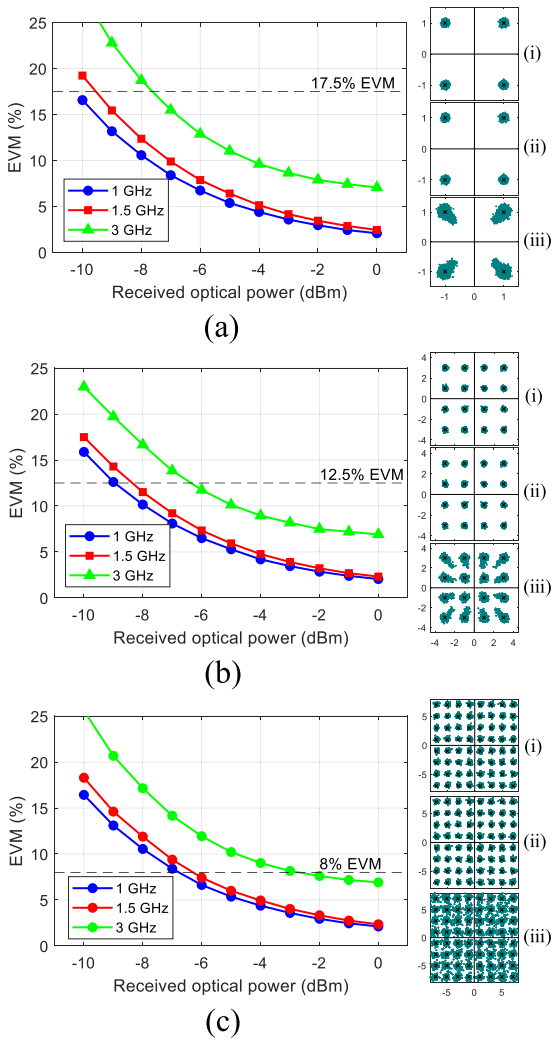

FIGURE 3. Simulated OB2B EVM performance for different signal bandwidth for: (a) 4-QAM, (b) 16-QAM, and (c) 64-QAM. Insets (i), (ii) and (iii) show the obtained constellations at received optical power (RoP) of -4 dBm for 1, 1.5 and 3 GHz, respectively.

is requested in the minimum received optical power (RoP) when the bandwidth is extended from 1 to 1.5 GHz, whereas 2.7 dB more power is needed when the signal bandwidth is increased up to 3 GHz. Insets (i), (ii) and (iii) of Fig. 3(a) show the constellation of the signal at the received optical power of −4 dBm with corresponding EVM values of 4.4%, 5.1% and 9.6% for 1, 1.5 and 3 GHz, respectively. Note that the degradation in the OB2B measurement is significantly larger for 3 GHz bandwidth signal due to the DML nonlinear response, which causes intermodulation distortions (IMD) [39]

The simulated results with EVM for 16-QAM are depicted in Fig. 3(b). As shown, lower data bandwidth leads the lowest EVM meanwhile higher data bandwidth undergoes stronger degradation. Compared to 1 GHz bandwidth, 0.6 and 2.6 dB higher optical power (i.e. power penalty) is required for 1.5 and 3 GHz bandwidths, respectively, in order to obtain similar performance. Constellations, obtained with −4 dBm of optical power, are shown in insets (i), (ii) and (iii) of Fig. 3(b), with EVM of 4.2%, 4.8% and 9.0%, respectively.

The 64-QAM EVM simulation results are shown in Fig. 3(c). As expected from previous results, larger bandwidths lead to higher EVM degradation also according to the channel transfer function depicted in Fig. 2. In this case, the optical power difference for 1.5 and 3 GHz respect to the 1 GHz signal bandwidth is 0.5 and 4 dB, respectively. However, the EVM performance is below 8% for optical received power higher than −2.7 dBm. The constellations shown in insets (i), (ii) and (iii) of Fig. 3(c) correspond to an EVM of 4.4%, 4.9% and 9%, respectively.

B. IMPACT OF FIBER DISPERSION ON 1 GHz 4/16/64-QAM

The evaluation of the impact of chromatic dispersion using a no-chirp DML in 4-, 16- and 64-QAM signal with 1 GHz bandwidth is shown in Fig. 4. Fig. 4(a) depicts the EVM of 4-QAM signal for OB2B, 10 and 20 km SSMF links, where penalties at EVM threshold (17.5%) can be determined as 0.4 and 1.4 dB for 10 and 20 km, respectively.

Fig. 4(b) depicts the simulated the same EVM performance for 16-QAM. In this case, the power penalty at EVM threshold (12.5%) is 1.4 and 3.7 dB for 10 and 20 km, respectively.

Finally, Fig. 4(c) shows the EVM performance for 64-QAM format, with a power penalty of 0.5 dB for 10 km SSMF at 8% EVM limit. However, this cannot be measured with 20 km since the EVM does not meet the 8% EVM limit requirement in the RoP range under study. All cases illustrate the impact of fiber dispersion on the channel transfer function, where system bandwidth is reduced for longer links, as shown in Fig. 2.

The constellations of 4-, 16- and 64-QAM simulated recovered data for different fiber lengths at RoP of −4 dBm, are shown in Fig. 5. Clear constellations are shown after 10 km transmission, which are similar to those corresponding to OB2B (see insets (i) in Fig. 3) whereas 20 km transmission leads to a larger spread, which is more severe for the outer symbols, as can be observed in 16-QAM constellation. Nevertheless, the degradation of the EVM is significant, as shown on the right side of Fig. 5(a), (b) and (c), which correspond to 4-, 16- and 64-QAM signal propagation over 20 km fiber with 10.3%, 10.1% and 10.5%, respectively. Nonlinear distortion is clearly observed due to the interplay between the DML nonlinear response and the fiber chromatic dispersion [39].

C. IMPACT OF DML CHIRP ON 1 GHz 4/16/64-QAM

In the following, chirp is also considered in the 1 GHz bandwidth signal transmission over 10 km SSMF link to evaluate the overall impact of the interplay of chirp and dispersion on the quality of the received signal. Based on commercial DMLs [17], different chirp values have been employed in the simulated schemes, as detailed in Table 1, and the results are illustrated in Fig. 6, where $\alpha = 1$ was employed for the calculations with non-zero chirp. Fig. 6(a) shows there is no power penalty at 17.5% EVM level when a DML

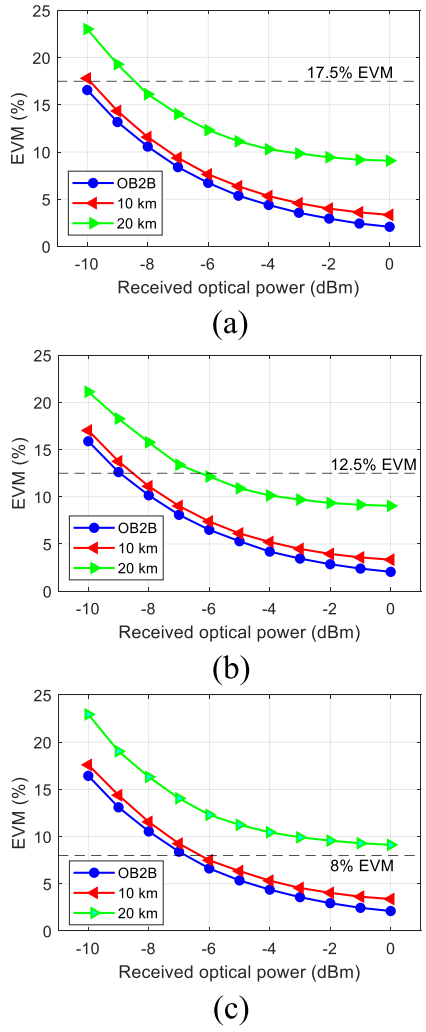

FIGURE 4. Simulated EVM performance after OB2B, 10 and 20 km SSMF link with 1 GHz signal bandwidth for different modulations: (a) 4-QAM, (b) 16-QAM and (c) 64-QAM.

with low chirp characteristic (4 GHz/mW) is modulated by the 4-QAM signal. However, moderate (10 GHz/mW) and high (15 GHz/mW) chirp values lead to penalties of 0.4 and 1 dB, respectively. Insets (i), (ii) and (iii) of Fig. 6(a) show the constellations of the recovered signals with -4 dBm of RoP, where obtained EVMs are 5.5%, 8.1% and 11.1% after 10 km fiber transmission with low, moderate and high chirped signals, respectively.

Fig. 6(b) shows the impact of the chirp when the 16-QAM signal with 1 GHz bandwidth is transmitted along 10 km SSMF. Similarly to the previous case, there is no power penalty when low chirp DML is employed signal at threshold EVM level, but the required RoP is increased by 0.8 and 2.6 dB for moderate and high chirp parameters, respectively. Constellations at −3 dBm RoP are shown in insets (i), (ii) and (iii) of Fig. 6(b).

Fig. 6(c) depicts the simulated EVM for 64-QAM signals. As shown, there is no difference between non- and low chirped signals at 8% limit. However, in this case,

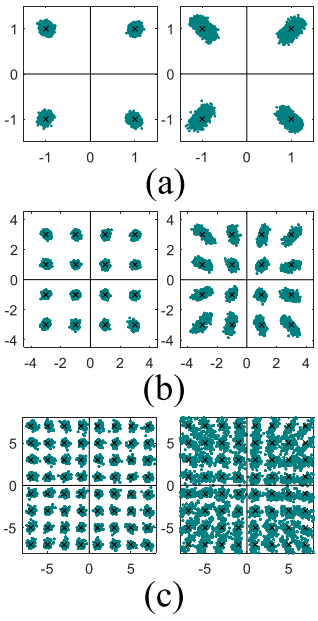

FIGURE 5. Constellations at RoP of -4 dBm for 1 GHz signal bandwidth: (a) 4-QAM, (b) 16-QAM and (c) 64-QAM. Constellations for 10 km (left side) and 20 km (right side) SSMF links, respectively.

the obtained EVM values are larger than 8% threshold limit when moderate and high chirp lasers are applied. Constellations in insets (i), (ii) and (iii) of Fig. 6(c) show the significant degradation of the received signal caused by the interplay of fiber dispersion and chirp, resulting in rotation with respect to the corresponding constellations obtained in Fig. 5. In accordance with this, the impact of the chirp was observed in the system transfer function depicted in Fig. 2. Therefore, the chirp in DML has a crucial influence on transmission characteristics, especially when higher-order modulation formats, i.e. 64-QAM, with high bandwidth are applied in such a network.

III. EXPERIMENTAL SETUP

The experimental system emulates the optical transceiver at the BBU in the central office (CO), as depicted in Fig. 7, which consists of a low chirp DML and an external MZM where the optical carrier modulated by data is upconverted before signal transmission over a 10 km SSMF link. An extended transmission setup based on a hybrid link including 1.5 m FSO segment was also considered to test the optical wireless performance for the sake of increasing the network flexibility [40]. In this experiment, the distributed feedback laser emitting an optical signal at 1553 nm with 5.7 dBm optical power was directly modulated by a M-QAM signal at intermediate frequency (IF) of 2 GHz generated by the data signal generator (DG) (Tektronix AWG7122C). The laser modulation response (see inset of Fig. 7) exhibits a −3 dB bandwidth of 6.2 GHz. The optical spectrum at the laser output (P1 in Fig. 7) was measured by a high resolution

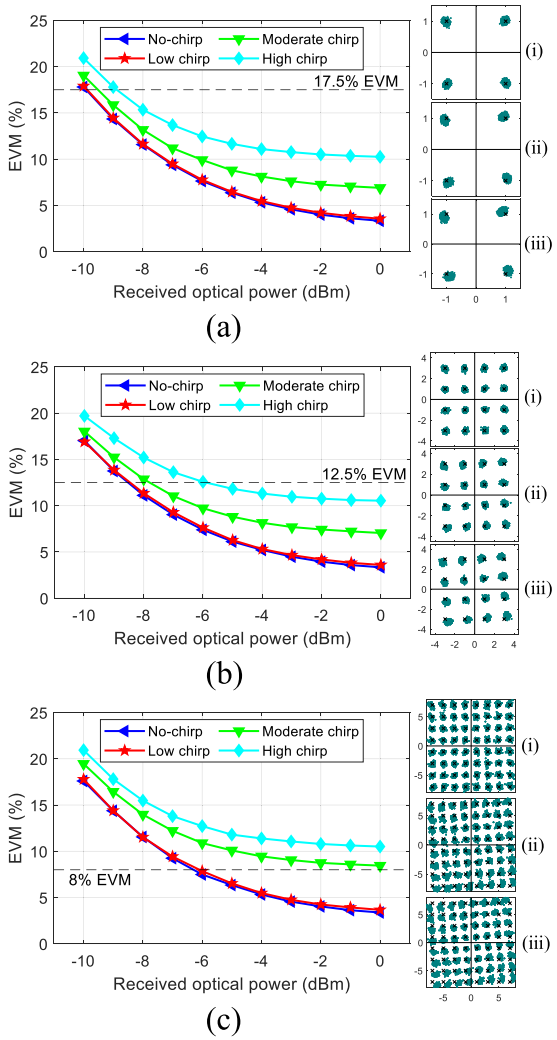

FIGURE 6. Simulated EVM performance when DML is employed with null, low, moderate and high chirp and 1 GHz signal bandwidth is transmitted over 10 km SSMF: (a) 4-QAM, (b) 16-QAM and (c) 64-QAM. Insets (i), (ii) and (iii) show constellations for low, moderate and high chirp value, respectively, at RoP of −3 dBm.

optical spectrum analyzer (OSA) (Aragon Photonics BOSA-PHASE, RBW = 0.08 pm), as depicted in Fig. 8(a) when a 16-QAM signal data with 200 MHz bandwidth was transmitted. It shows an optical carrier to band ratio of 22.3 dB, i.e. an equivalent DML modulation index of 15% and an optical signal-to-noise ratio (OSNR) of 63.4 dB.

After adjusting the polarization state of the optical signal by a polarization controller (PC), it was launched into the MZM (Photline MX-LN-40), which was driven by a 20 GHz and 18 dBm signal clock generated by a signal generator (SG) (Agilent 8267C) and biased at null transmission point (V_π), i.e. 1.3 V, to obtain the optical carrier suppression. The optical spectrum of the modulated signal (P2 in Fig. 7) is displayed in Fig. 8(b). The side-mode suppression ratio (SMSR) between the carrier and sidebands is measured as 37.4 dB. An erbium doped fiber amplifier (EDFA) (Amonics AEDFA-23-B-FA) with 13 dBm constant output power was employed to compensate for the optical losses. The amplified spontaneous emission (ASE) noise was filtered out by an optical band pass filter (OBPF) (Alnair BVF-100) with $\Delta\lambda = 2$nm.

In the experiment, a single-tone was employed in DML to measure the channel response as the S21 scattering parameter. Fig. 9 shows the OB2B measurement where the −3 dB bandwidth limitation of 5 GHz is due to the transmitter and receiver constraints. However, as explained in the previous section, the transmission over a given length of dispersive fiber leads to a channel response with several notches limiting the operating bandwidth. More specifically, the measured channel response of 10 km fiber link shows a 3 dB bandwidth of 1.2 GHz and the notch appears close to 6 GHz, whereas notches at 2.4 and 1.7 GHz appear when signals are transmitted over 25 and 35 km fiber links, respectively, as indicated from (2) and (3) when k= 1 GHz/mW and $\alpha = 0.55$ (dotted lines correspond to theoretical response in Fig. 9).

The system performance with data was characterized for the OB2B, a 10 km SSMF link and finally, for a hybrid link composed of 10 km SSMF and 1.5 m FSO channel emulating the ODN between the BBU and the RRH. In the latter, focusing the beam was achieved by using graded-index lenses (GRIN) (Thorlabs 50-1550A-APC) with an aperture of 1.8 mm and plano-convex lenses with a diameter of 25.4 mm. Note that the measured FSO losses were 6.5 dB and therefore another EDFA (Amonics AEDFA-27-B-FA) with 13 dBm constant output power and OBPF (Waveshaper 4000S) with $\Delta\lambda = 2$ nm was needed.

At the RRH side, the optical signal was captured by the PD (u2t BPDV2020R, 40 GHz bandwidth), where 40 GHz electrical signal was generated by beating the first-order sidebands at the PD. Finally, the electrical signal was amplified by an electrical RF amplifier (EA) (SHF Comm. Tech. AG SHF-810) with 29 dB gain, and analysed by a RF spectrum analyzer (RFSA) (Agilent N9020A, 26.5 GHz bandwidth) and a digital phosphor oscilloscope (DPO) (Tecktronix DPO72004C). Fig. 10 depicts the electrical spectrum measured by a RFSA when 500 MHz bandwidth, corresponding to the maximum considered single channel bandwidth in bands above 24 GHz for 5G [41], when 16-QAM data signal is transmitted along the OB2B link. The upper data band shows higher degradation than the lower one due to the PD frequency response. The averaged electrical power of lower band is −50 dBm, where nonlinearities and noise floor at −68 dBm can be observed in the electrical RF spectrum. In the next section, we will investigate the EVM performance of the proposed system for a wide range of RoP from −3 to 6 dBm. This measurement is essential in order to determine the system dynamic range and an appropriate RoP level considering the mmW link for practical implementation. More concretely, according to Fig. 9, there is a 5 dB penalty due to 10 km SMF at the working frequency, which can be demonstrated to be reasonable for the base station since the adequate RoP regime prevents from nonlinear limited region of the EA.

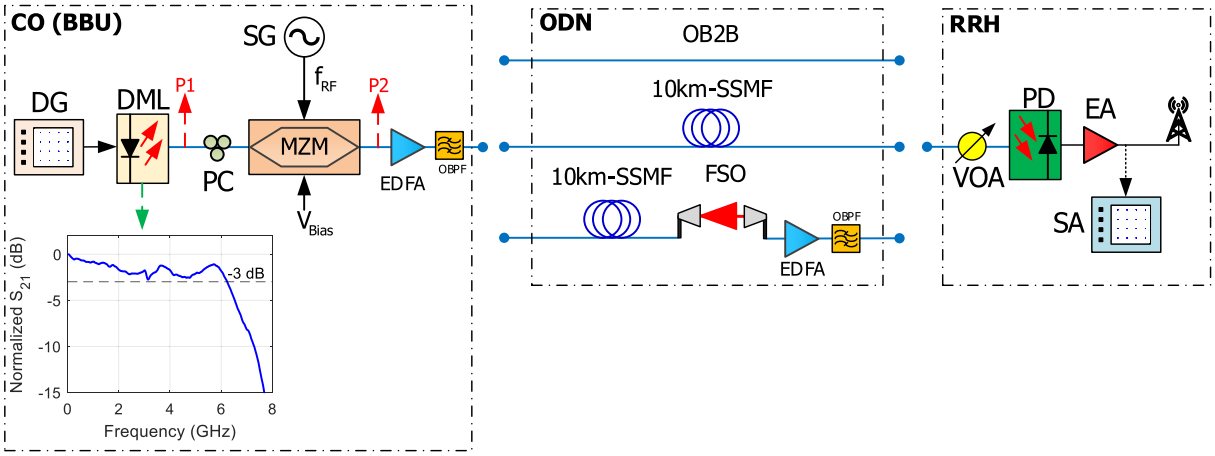

FIGURE 7. Experimental setup. Inset shows the electro-optical response of DML. CO: central office, BBU: baseband unit, RRH: remote radio head, ODN: optical distribution network, DG: data generator, DML: directly-modulated laser, PC: polarization controller, SG: signal generator, MZM: Mach Zehnder modulator, EDFA: erbium doped fiber amplifier, OBPF: optical band pass filter, OB2B: optical back-to-back, SSMF: standard single mode fiber, FSO: free space optics, VOA: variable optical attenuator, PD: photodetector, EA: electrical amplifier, SA: signal analyzer.

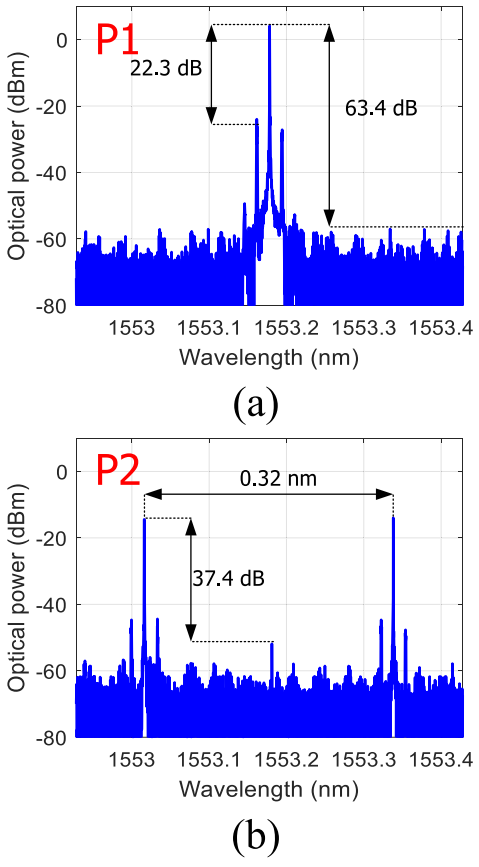

FIGURE 8. Optical spectra of: (a) signal emitted by the DML and (b) modulated signal (RBW = 0.08 pm).

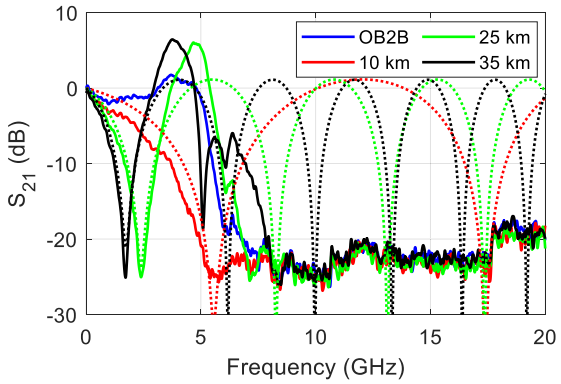

FIGURE 9. Measured single-tone channel frequency response for different fiber lengths. Dotted lines are calculated from (2) and (3) with $k = 1$ GHz/mW and $\alpha = 0.55$.

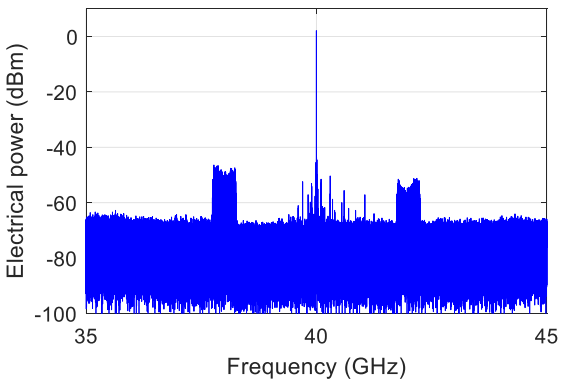

FIGURE 10. Electrical spectrum of 16-QAM data signal with 500 MHz bandwidth at 40 GHz mmW along OB2B link (RBW = 51 kHz, VBW = 51 kHz).

IV. TRANSMISSION RESULTS

The system performance was evaluated by using 4-,16- and 64-QAM signals with bandwidth from 50 MHz up to 1000 MHz at 40 GHz carrier frequency and 2 GHz IF. Fig. 11 shows the measured EVM of the recovered signals when 4-QAM format was employed. Fig. 11(a) then shows the OB2B where, as expected, larger bandwidths

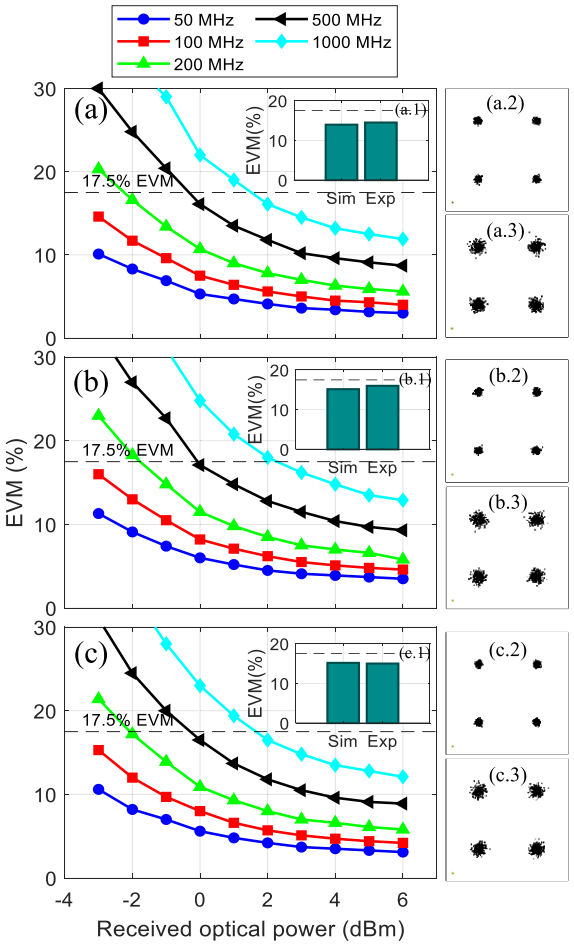

FIGURE 11. Measured EVM of 4-QAM for different signal bandwidths: (a) OB2B, (b) SSMF and (c) Hybrid links. Insets (a.1), (b.1) and (c.1) show the comparison between simulation and experimental results for 1 GHz and 3 dBm RoP. Constellations for 3 dBm RoP: (a.2), (b.2) and (c.2) with 100 MHz bandwidth, and (a.3), (b.3) and (c.3) with 500 MHz bandwidth.

lead to higher EVM values in fiber and hybrid links (Fig. 11(b)) and (c), respectively).Note that insets (a.1), (b.1) and (c.1) show very good agreement with theoretical simulations obtained using a DML with chirp k= 1 GHz/mW and α = 0.55 (see Figure 9) for 1 GHz bandwidth and 3 dBm RoP. Nevertheless, the reliable transmission is achieved for the 4-QAM under 17.5% EVM threshold limit. The power penalty due to 10 km fiber link is below 0.6 dB for bandwidths 100 and 200 MHz, i.e. 0.3 and 0.6 dB, respectively, and it increases up to 0.8 dB for 1000 MHz. The standard EVM threshold level is satisfied with -0.3 and 1.5 dBm optical power after SSMF transmission for 500 and 1000 MHz bandwidth, respectively. EVM measurements were also done after transmission along a hybrid link composed of a 10 km SSMF and 1.5 m FSO link showing no significant penalties introduced by the hybrid link (Fig. 11(c)). Insets in Fig. 11 show the constellations of received signals with 3 dBm received optical power where degradation due to fiber link is observed to be almost negligible. Indeed, insets (a.3), (b.3) and (c.3), correspond to larger bandwidth and thus show larger degradation, however EVM values are kept below the standard EVM limit for all signals having a received optical power at least of 2 dBm.

The 16-QAM signals with 50 to 500 MHz bandwidth were also transmitted in our experimental setup and measured EVM values are shown in Fig. 12. For OB2B (Fig. 12(a)), a received optical power of −3 dBm for 50 MHz is required to satisfy the 12.5% EVM threshold meanwhile the optical power is increased up to 3 dBm for 500 MHz bandwidth. The penalty due to the fiber dispersion increases with the bandwidth (Fig. 12(b)), from 0.5 dB for 50 MHz to 1 dB for 500 MHz. Again, transmission over the hybrid link did not lead to additional penalties, as shown in Fig. 12(b). The constellations of 100 MHz bandwidth with 6 dBm received optical power (insets (i), (iii) and (v)) show low degradation due to fiber transmission meanwhile 500 MHz bandwidth (insets (ii), (iv) and (vi)) leads to higher degradation. However, a successful signal transmission has been demonstrated in all cases.

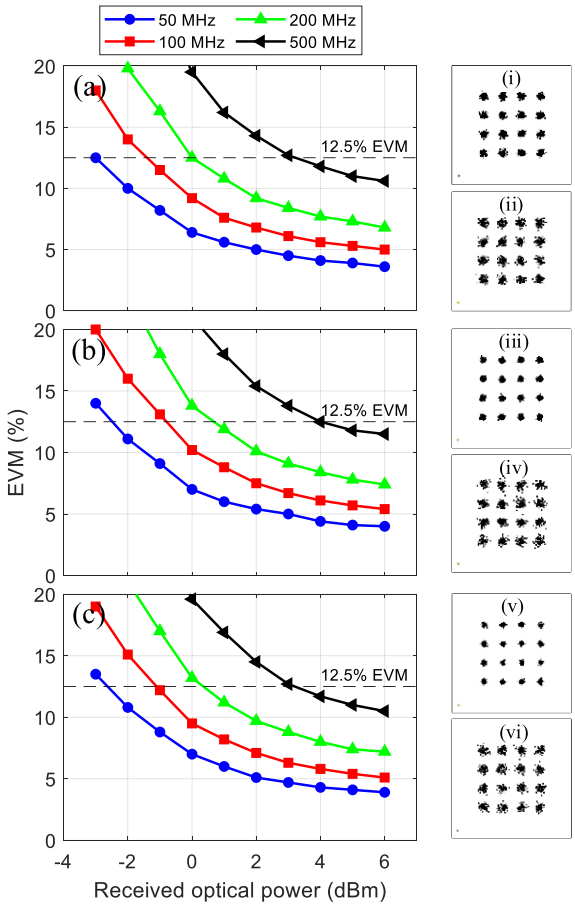

FIGURE 12. Measured EVM of 16-QAM for different signal bandwidths: (a) OB2B, (b) SSMF and (c) Hybrid links. Insets show the constellations when 6 dBm received optical power: (i), (iii) and (iv) with 100 MHz bandwidth, and (ii), (v) and (vi) with 500 MHz bandwidth.

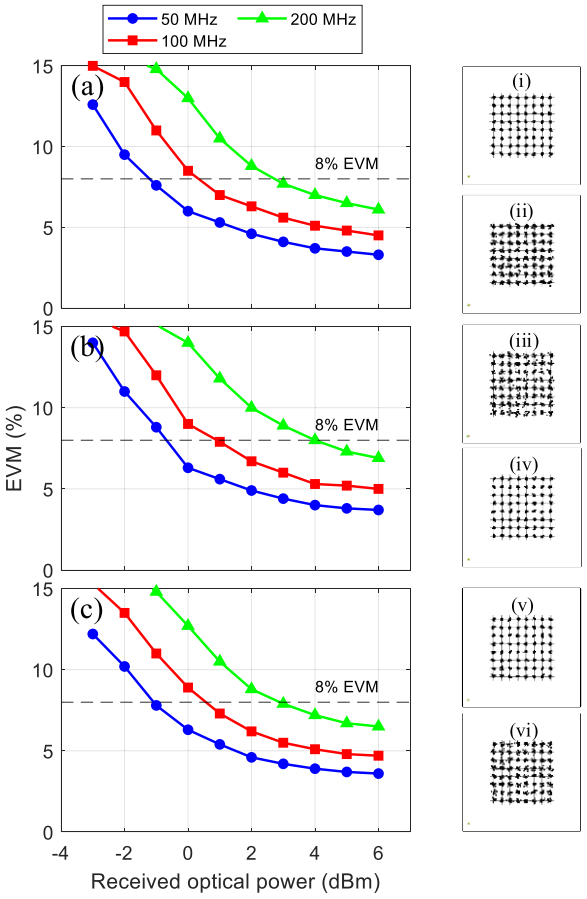

FIGURE 13. Measured EVM of 64-QAM for different signal bandwidths: (a) OB2B, (b) SSMF and (c) Hybrid links. Insets show the constellations when 6 dBm received optical power: (i), (iii) and (iv) with 50 MHz bandwidth, and (ii), (v) and (vi) with 200 MHz bandwidth.

Finally, Fig. 13 shows the EVM results when 64-QAM signals with different bandwidths are transmitted. OB2B measurements are shown in Fig. 13(a). The EVM is kept below 8% when received optical power is higher than -1.5, 0.5 and 2.9 dBm for 50, 100 and 200 MHz, respectively. The power penalty due to the SSMF (Fig. 13(b)) is 0.3, 0.6 and 1.1 dB for 50, 100 and 200 MHz, respectively. As expected, there is no additional significant penalty due to the FSO link. Again, constellations of 50 MHz (insets (i), (iii) and (iv)) exhibit lower degradation than the constellation of 200 MHz for all links (insets (ii), (iv) and (vi)), nevertheless the EVM lower than 8% for 64-QAM and 200 MHz bandwidth has been achieved.

According to the experimental measurements, Fig. 14 shows the bitrate in terms of the minimum RoP required to satisfy EVM below the 3GPP limits for 4-, 16- and 64-QAM, respectively, for different data bandwidth. Note that the displayed throughput results correspond to bandwidth from 50 to 1000 MHz for 4-QAM, 50 to 500 MHz for 16-QAM and 50 to 200 MHz for 64-QAM. As expected, 4-QAM signals

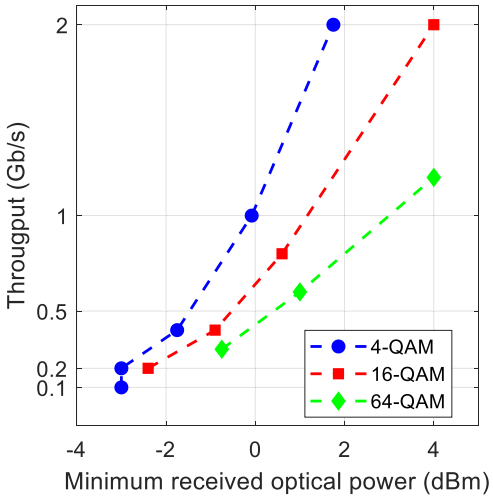

FIGURE 14. Data throughput obtained from bandwidth results in Fig. 11, 12 and 13 vs minimum RoP for 10 km SSMF link at EVM limit.

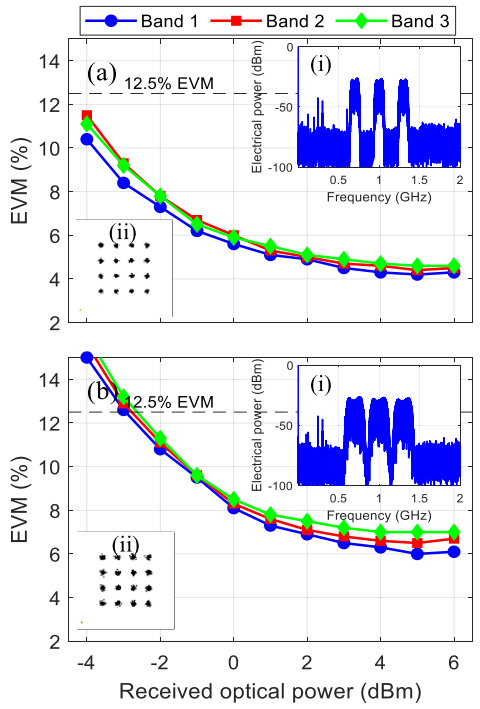

FIGURE 15. EVM of 16-QAM multiband data signal over 10 km fiber link with: (a) 100 MHz and (b) 200 MHz bandwidth. Insets: (i) Electrical spectra of multiband signal ("RBW = 100 kHz", "VBW = 100 kHz"), (ii) Constellations of band 2 with 3 dBm RoP.

support larger bandwidth than 16- and 64-QAM signals. The minimum RoP for 4-QAM providing maximal bit rate, i.e. 2 Gb/s at 1000 MHz bandwidth, is 1.8 dBm meanwhile 4 dBm is needed for 2Gb/s (500 MHz bandwidth) and 1.2 Gb/s (200 MHz bandwidth) under 16- and 64-QAM modulation formats, respectively. In other words, to achieve e.g. 2 Gb/s throughput, it is possible to employ either 4-QAM with 1000 MHz bandwidth or 16-QAM with 500 MHz bandwidth, although 2.2 dB higher received optical power is required in the latter case.

V. MULTIBAND TRANSMISSION

After demonstrating the bandwidth usability of low cost DML for signal transmission over photonically mmW generated signals, this section proposes to fully exploit the available bandwidth of the components, in spite of dispersion and chirp penalties, by using a multiband transmission approach [13]. Three bands with same bandwidth at 0.7, 1.0 and 1.3 GHz were transmitted using 16-QAM format and EVM measurements were done with 100 and 200 MHz bandwidth of each band.

In this part, the setup depicted in Fig. 7 is slightly modified and optimized for multiband data transmission. The multiband signal is amplified by 9 dB before launched into the DML. The baseband electrical spectrum generated for 100 and 200 MHz 16-QAM data signal is shown as insets (i) in Fig. 15(a) and (b), respectively. After the optical transmission and opto-electronic conversion at PD, the generated electrical signal is also amplified by 40 dB before the signal analyzer.

The EVM measurements corresponding to the three bands are shown in Fig. 15 (see constellations of band 2 with RoP of 3 dBm in the inset (ii)). Fig. 15(a) shows the EVM measurements corresponding to three bands with 100 MHz data bandwidth. EVM values are kept below the standard EVM limit for all bands within the RoP range under measurement and there is only a slight difference between frequency bands. EVM measurements obtained with 200 MHz 16-QAM multibands signal are slightly higher, as shown in Fig. 15(b), and in any case, the EVM is below the EVM threshold with RoP higher than −3 dBm.

VI. CONCLUSION

A cost-effective mmW 5G mobile optical fronthaul operating at 40 GHz has been comprehensively investigated in both simulation analysis and experimental demonstrations to transmit single and multiband M-QAM signals. A DML and an external modulator for optical frequency multiplication under a carrier suppressed modulation scheme have been employed. The simulation results allow to determine the combined effect of the chirp and fiber dispersion and its impact on the signal bandwidth and the system performance. Different values of chirp and fiber lengths, as well as different signal bandwidths have been considered, and penalties of 1, 2.3 and 6 dB have been identified for 4-, 16- and 64-QAM formats between non- and high chirp, respectively. In the experimental setup, a low chirp commercial DML was employed and M-QAM signals with bandwidths from 50 to 1000 MHz were transmitted along 10 km SSMF and 1.5 m FSO channel, while 1 dBm of received optical power was required for 1000, 500 and 200 MHz bandwidths (i.e. 2, 2 and 1.2 Gb/s) using 4-, 16- and 64- QAM, respectively. From another perspective, we have demonstrated a fronthaul solution connecting centralized BBU and RRH operating in hybrid fiber/FSO network with bit rates achieving from 1.2 to 2 Gb/s occupying bandwidths from 200 to 1000 MHz depending on particular QAM format to fulfil high data throughput requirements for 5G MFN in mmW frequency spectrum. Finally, multiband signal transmission has been implemented to increase the bandwidth usability while maintaining reduced costs and therefore, the potentiality of such systems are demonstrated towards future massive deployment of 5G networks. Experimental measurements also show the feasibility of including free-space optics links in the optical distribution network with no further significant penalties.

REFERENCES

[1] A. Ghosh, A. Maeder, M. Baker, and D. Chandramouli, "5G evolution: A view on 5G cellular technology beyond 3GPP release 15," *IEEE Access*, vol. 7, pp. 127639–127651, 2019.

[2] C. Lim, Y. Tian, C. Ranaweera, T. A. Nirmalathas, E. Wong, and K.-L. Lee, "Evolution of Radio-Over-Fiber technology," *J. Lightw. Technol.*, vol. 37, no. 6, pp. 1647–1656, Mar. 15, 2019.

[3] C. Ranaweera, E. Wong, A. Nirmalathas, C. Jayasundara, and C. Lim, "5G C-RAN with optical fronthaul: An analysis from a deployment perspective," *J. Lightw. Technol.*, vol. 36, no. 11, pp. 2059–2068, Jun. 1, 2018.

[4] S. T. Le, T. Drenski, A. Hills, M. King, K. Kim, Y. Matsui, and T. Sizer, "400Gb/s real-time transmission supporting CPRI and eCPRI trafc for hybrid LTE-5G networks," in *Proc. Opt. Fiber Commun. Conf. Exhib. (OFC)*, Mar. 2020, pp. 1–3, Paper Th4C-4.

[5] Y. Zhu, Y. Wu, H. Xu, C. Browning, L. P. Barry, and Y. Yu, "Experimental demonstration of a WDM-RoF based mobile fronthaul with f-OFDM signals by using directly modulated 3s-DBR laser," *J. Lightw. Technol.*, vol. 37, no. 16, pp. 3875–3881, Aug. 15, 2019.

[6] "Radio-over-fibre (RoF) technologies and their applications, Series G suplement 55," Tech. Rep., ITU-T, 2015. [Online]. Available: https://www.itu.int/rec/dologin_pub.asp?lang=e&id=T-REC-G.Sup55-201507-I!!PDF-E&type=items

[7] H. Schmuck, R. Heidemann, and R. Hofstetter, "Distribution of 60 GHz signals to more than 1000 base stations," *Electron. Lett.*, vol. 30, no. 1, pp. 59–60, Jan. 1994.

[8] X. Pang, A. Caballero, A. Dogadaev, V. Arlunno, L. Deng, R. Borkowski, J. S. Pedersen, D. Zibar, X. Yu, and I. Tafur Monroy, "25 Gbit/s QPSK hybrid fiber-wireless transmission in the W-band (75–110 GHz) with remote antenna unit for in-building wireless networks," *IEEE Photon. J.*, vol. 4, no. 3, pp. 691–698, Jun. 2012.

[9] R. Puerta, J. Yu, X. Li, Y. Xu, J. J. Vegas Olmos, and I. T. Monroy, "Single-carrier dual-polarization 328-Gb/s wireless transmission in a D-band millimeter wave 2 × 2 MU-MIMO radio-over-fiber system," *J. Lightw. Technol.*, vol. 36, no. 2, pp. 587–593, Jan. 15, 2018.

[10] H.-Y. Wang, C.-H. Cheng, C.-T. Tsai, Y.-C. Chi, and G.-R. Lin, "Multi-color laser diode heterodyned 28-GHz millimeter-wave carrier encoded with DMT for 5G wireless mobile networks," *IEEE Access*, vol. 7, pp. 122697–122706, 2019.

[11] A. Chowdhury, H.-C. Chien, S.-H. Fan, J. Yu, and G.-K. Chang, "Multi-band transport technologies for in-building host-neutral wireless over fiber access systems," *J. Lightw. Technol.*, vol. 28, no. 16, pp. 2406–2415, Aug. 15, 2010.

[12] Y.-T. Hsueh, Z. Jia, H.-C. Chien, A. Chowdhury, J. Yu, and G.-K. Chang, "Multiband 60-GHz wireless over fiber access system with high dispersion tolerance using frequency tripling technique," *J. Lightw. Technol.*, vol. 29, no. 8, pp. 1105–1111, Apr. 2011.

[13] M. Mohamed, X. Zhang, B. Hraimel, and K. Wu, "Optical generation of millimeter-wave multiband OFDM ultra-wideband wireless signal and distribution over fiber," *IEEE Photon. Technol. Lett.*, vol. 22, no. 15, pp. 1180–1182, Aug. 2010.

[14] Z. Tang, F. Zhang, and S. Pan, "60-GHz RoF system for dispersion-free transmission of HD and multi-band 16 QAM," *IEEE Photon. Technol. Lett.*, vol. 30, no. 14, pp. 1305–1308, Jul. 15, 2018.

[15] P. T. Dat, A. Kanno, N. Yamamoto, and T. Kawanishi, "Seamless convergence of fiber and wireless systems for 5G and beyond networks," *J. Lightw. Technol.*, vol. 37, no. 2, pp. 592–604, Nov. 2019.

[16] K. Van Gasse, J. Van Kerrebrouck, A. Abbasi, G. Torfs, H. Chen, X. Yin, J. Bauwelinck, and G. Roelkens, "480 Mbps/1 gbps radio-over-fiber link based on a directly modulated III-V-on-silicon DFB laser," in *Proc. IEEE Int. Topical Meeting Microw. Photon. (MWP)*, Nov. 2016, pp. 328–331.

[17] B. G. Kim, S. H. Bae, H. Kim, and Y. C. Chung, "RoF-based mobile fronthaul networks implemented by using DML and EML for 5G wireless communication systems," *J. Lightw. Technol.*, vol. 36, no. 14, pp. 2874–2881, Jul. 15, 2018.
[18] J. Bohata, M. Komanec, J. Spáčil, Z. Ghassemlooy, S. Zvánovec, and R. Slavík, "24–26 GHz radio-over-fiber and free-space optics for fifth-generation systems," *Opt. Lett.*, vol. 43, no. 5, pp. 1035–1038, Mar. 2018.
[19] T. Shao, E. P. Martin, P. M. Anandarajah, and L. P. Barry, "60-GHz direct modulation-direct detection OFDM-RoF system using gain-switched laser," *IEEE Photon. Technol. Lett.*, vol. 27, no. 2, pp. 193–196, Jan. 15, 2015.
[20] C. Vagionas, H. Debregeas, G. Kalfas, N. Pleros, S. Papaioannou, N. Argyris, K. Kanta, N. Iliadis, G. Giannoulis, D. Apostolopoulos, H. Avramopoulos, and C. Caillaud, "A 6-band 12Gb/s IFoF/V-band fiber-wireless fronthaul link using an InP externally modulated laser," in *Proc. Eur. Conf. Opt. Commun. (ECOC)*, Sep. 2018, pp. 1–3.
[21] J. Bohata, M. Komanec, J. Spacil, R. Slavik, and S. Zvanovec, "Transmitters for combined radio over a fiber and outdoor millimeter-wave system at 25 GHz," *IEEE Photon. J.*, vol. 12, no. 3, pp. 1–14, Jun. 2020.
[22] M. S. B. Cunha, E. S. Lima, N. Andriolli, D. H. Spadoti, G. Contestabile, and A. Cerqueira, "5G NR RoF system based on a monolithically integrated multi-wavelength transmitter," *IEEE J. Sel. Topics Quantum Electron.*, vol. 27, no. 2, pp. 1–8, Mar. 2021.
[23] M. J. Fice, E. Rouvalis, F. van Dijk, A. Accard, F. Lelarge, C. C. Renaud, G. Carpintero, and A. J. Seeds, "146-GHz millimeter-wave radio-over-fiber photonic wireless transmission system," *Opt. Exp.*, vol. 20, no. 2, pp. 1769–1774, 2012.
[24] L. Gan, J. Liu, F. Li, and P. K. A. Wai, "An optical millimeter-wave generator using optical higher order sideband injection locking in a Fabry–Pérot laser diode," *J. Lightw. Technol.*, vol. 33, no. 23, pp. 4985–4996, Dec. 1, 2015.
[25] M. Hyodo, S. Saito, and Y. Kasai, "Optical phase-locked loop with fibre lasers for low phase noise millimetre-wave signal generation," *Electron. Lett.*, vol. 45, no. 17, p. 878, 2009.
[26] P.-T. Shih, J. Chen, C.-T. Lin, W.-J. Jiang, H.-S. Huang, P.-C. Peng, and S. Chi, "Optical millimeter-wave signal generation via frequency 12-tupling," *J. Lightw. Technol.*, vol. 28, no. 1, pp. 71–78, Jan. 2010.
[27] Y.-K. Seo, C.-S. Choi, and W.-Y. Choi, "All-optical signal up-conversion for radio-on-fiber applications using cross-gain modulation in semiconductor optical amplifiers," *IEEE Photon. Technol. Lett.*, vol. 14, no. 10, pp. 1448–1450, Oct. 2002.
[28] T. Schneider, M. Junker, and D. Hannover, "Generation of millimetre-wave signals by stimulated Brillouin scattering for radio over fibre systems," *Electron. Lett.*, vol. 40, no. 23, pp. 295–304, 2004.
[29] H. Zhang, L. Cai, S. Xie, K. Zhang, X. Wu, and Z. Dong, "A novel radio-over-fiber system based on carrier suppressed frequency eightfold millimeter wave generation," *IEEE Photon. J.*, vol. 9, no. 5, pp. 1–6, Oct. 2017.
[30] X. Liu and F. Effenberger, "Emerging optical access network technologies for 5G wireless," *J. Opt. Commun. Netw.*, vol. 8, no. 12, pp. B70–B79, 2016.
[31] L. Zhang, M. Zhu, C. Ye, S.-H. Fan, C. Liu, X. Hu, P. Cao, Q. Chang, Y. Su, and G.-K. Chang, "Generation and transmission of multiband and multi-gigabit 60-GHz MMW signals in an RoF system with frequency quintupling technique," *Opt. Exp.*, vol. 21, no. 8, p. 9899, 2013.
[32] C.-T. Lin, J. J. Chen, S.-P. Dai, P.-C. Peng, and S. Chi, "Impact of nonlinear transfer function and imperfect splitting ratio of MZM on optical up-conversion employing double sideband with carrier suppression modulation," *J. Lightw. Technol.*, vol. 26, no. 15, pp. 2449–2459, Aug. 2008.
[33] L. Chen, S. C. Wen, Y. Li, J. He, H. Wen, Y. Shao, Z. Dong, and Y. Pi, "Optical front-ends to generate optical millimeter-wave signal in radio-over-fiber systems with different architectures," *J. Lightw. Technol.*, vol. 25, no. 11, pp. 3381–3387, Nov. 2007.
[34] X. Li, J. Xiao, Y. Xu, L. Chen, and J. Yu, "Frequency-doubling photonic vector millimeter-wave signal generation from one DML," *IEEE Photon. J.*, vol. 7, no. 6, pp. 1–7, Dec. 2015.
[35] C.-T. Tsai, C.-H. Lin, C.-T. Lin, Y.-C. Chi, and G.-R. Lin, "60-GHz millimeter-wave over fiber with directly modulated dual-mode laser diode," *Sci. Rep.*, vol. 6, no. 1, p. 27919, Jun. 2016.
[36] L. Anet Neto, D. Erasme, N. Genay, P. Chanclou, Q. Deniel, F. Traore, T. Anfray, R. Hmadou, and C. Aupetit-Berthelemot, "Simple estimation of fiber dispersion and laser chirp parameters using the downhill simplex fitting algorithm," *J. Lightw. Technol.*, vol. 31, no. 2, pp. 334–342, Jan. 2013.
[37] K. Zhang, Q. Zhuge, H. Xin, W. Hu, and D. V. Plant, "Performance comparison of DML, EML and MZM in dispersion-unmanaged short reach transmissions with digital signal processing," *Opt. Exp.*, vol. 26, no. 26, pp. 34288–34304, 2018.
[38] "User equipment (UE) radiotransmission and reception; part 2: Range 2 standalone," ETSI, Sophia Antipolis, France, Tech. Rep. TS 138.101-1 V15.5.0, 2019. [Online]. Available: https://www.etsi.org/deliver/etsi_ts/138100_138199/13810101/15.05.00_60/ts_13810101v150500p.pdf
[39] C. Sánchez, B. Ortega, J. L. Wei, J. Tang, and J. Capmany, "Analytical formulation of directly modulated OOFDM signals transmitted over an IM/DD dispersive link," *Opt. Exp.*, vol. 21, no. 6, pp. 7651–7666, 2013.
[40] R. Zhang, F. Lu, M. Xu, S. Liu, P.-C. Peng, S. Shen, J. He, H. J. Cho, Q. Zhou, S. Yao, and G.-K. Chang, "An ultra-reliable MMW/FSO A-RoF system based on coordinated mapping and combining technique for 5G and beyond mobile fronthaul," *J. Lightw. Technol.*, vol. 36, no. 20, pp. 4952–4959, Oct. 15, 2018.
[41] *5G Spectrum*, GSMA Public Policy Position, London, U.K., 2020.

LUIS VALLEJO (Member, IEEE) was born in Malaga, Andalucia, Spain, in 1991. He received the B.Sc. degree in telecommunication technology engineering and the M.Sc. degree in telecommunication engineering from the Universidad de Malaga, Spain, in 2016 and 2017, respectively. He is currently pursuing the Ph.D. degree in telecommunication engineering program with the Universitat Politecnica de Valencia (UPV), Spain. He did a Test and Verification Engineer Internship with Keysight Technologies in 2017. He joined the Instituto de Telecomunicaciones y Aplicaciones Multimedia (iTEAM), Photonic Research Labs (PRL), UPV, in 2018. His research interests include microwave photonics, mmW generation, RoF/FSO for 5G and beyond, and optical access networks.

BEATRIZ ORTEGA (Member, IEEE) received the M.Sc. degree in physics from the Universidad de Valencia, in 1995, and the Ph.D. degree in telecommunications engineering from the Universidad Politécnica de Valencia, in 1999. She currently works with the Departamento de Comunicaciones, Universitat Politècnica de València, where she also holds a Full Professorship since 2009 and collaborates as a Group Leader with the Photonics Research Labs, Institute of Telecommunications and Multimedia Applications. She has published more than 200 articles and conference contributions in fibre Bragg gratings, microwave photonics, and optical networks. She has held several patents and is also a co-founder of EPHOOX company. She has participated in a large number of European Networks of Excellence and Research and Development projects and other national ones. Her main research interests include optical devices, optical networks, and microwave photonic systems and applications.

DONG-NHAT NGUYEN (Member, IEEE) received the B.Eng. (Hons.) and Ph.D. degrees in electrical engineering from the University of Nottingham, Malaysia Campus, Malaysia, in 2014 and 2018, respectively.

From Spring 2017 to Summer 2020, he was a Visiting Researcher with KAIST, Daejeon, South Korea, and UPV, Valencia, Spain, respectively. He is currently a Postdoctoral Researcher with Czech Technical University, Prague, Czech Republic. His research interests include the seamless convergence of RF/Fiber/FSO for 5G and beyond, optical access networks, advanced modulation formats, and signal processing.

JAN BOHATA was born in Prague, Czech Republic, in 1988. He received the B.S. and M.S. degrees in communications, electronics, and multimedia from the Faculty of Electrical Engineering, Czech Technical University, Prague, in 2012, and the Ph.D. degree in radio electronics, in 2018.

In 2012, he joined the Wireless and Fiber Optics Group, Department of Electromagnetic Field with a main focus on microwave photonics, fiber and free space optics networks, and optical communications in harsh environments. He is the author of more than 30 journal and conference papers and has been involved in a number of national and European research projects.

VICENÇ ALMENAR was born in Valencia, Spain, in 1969. He received the degree in telecommunications engineering and the Ph.D. degree from the Universitat Politècnica de València (UPV), in 1993 and 1999, respectively. In 2000, he did a Postdoctoral Research stay at the Centre for Communications Systems Research (CCSR), University of Surrey, U.K., where he was involved in research on digital signal processing for OFDM systems. He joined the Communications Department, UPV, in 1993, and became an Associate Professor in 2002 and a Professor in 2017. He was the Deputy Director of the department, from 2004 until 2014. His current research interests include OFDM, MIMO, and signal processing techniques for wireless and optical communications systems.

STANISLAV ZVANOVEC (Senior Member, IEEE) received the M.Sc. and Ph.D. degrees from the Faculty of Electrical Engineering, Czech Technical University (CTU), Prague, in 2002 and 2006, respectively. He is currently works as a Full Professor, the Deputy Head of the Department of Electromagnetic Field, and the Chairperson of the Ph.D. Branch with CTU. His current research interests include free space optical and fiber optical systems, visible light communications, OLED, RF over optics, and electromagnetic wave propagation issues for millimeter wave band. He is the author of two books (and coauthor of the recent book *Visible Light Communications: Theory and Applications*), several book chapters, and more than 250 journal articles and conference papers.